Optimal design of parallel manipulators based on their dynamic performance

Jagadeesh Kilaru*   Murali K Karnam†   Saurav Agarwal‡   Sandipan Bandyopadhyay§
Robotics Laboratory, Department of Engineering Design, Indian Institute of Technology Madras, TN, India - 600036.

Abstract—*This paper presents an approach for the design of parallel manipulators, from the perspective of optimal dynamic performance over a given safe working zone. It is shown that no single index is sufficient to fully quantify the dynamic performance of such a system. Two different indices are therefore developed from the study of the generic equation of motion of such systems. The resulting bi-objective optimisation problem is solved using a genetic algorithm-based numerical optimiser, namely, NSGA-II. The proposed algorithm is applied to an existing planar 3-<u>RRR</u> parallel manipulator, to obtain an improved design. It is found that the improved design, though obtained by optimising the intrinsic performance indices, perform better in terms of extrinsic dynamic indices, such as the required torque for tracking a set of given trajectories.*

Keywords: manipulator dynamics, parallel robots, optimisation, genetic algorithm

I. Introduction

A manipulator is typically designed for certain desirable features, such as a large workspace (in comparison to its dimensions) [1], good dynamic performance ([2], [3], [4]), dexterity [5], etc. The task of designing parallel manipulators presents many challenges. For example, the "workspace" needs to be qualified further as a subset of the actual workspace (termed as the *safe working zone* (SWZ) in [6]), which is free from singularity defects and link interferences, and needs to be identified at additional computational cost. On the other hand, it is difficult to find quantifiable measures of dynamic performance that can be used as design objectives. From a practical standpoint, a manipulator can be said to have "good" dynamic behaviour, when it can track trajectories without requiring high levels of forces/torques from its actuators, irrespective of the shape of the path, and its location in the workspace. This has a direct impact on the sizing of the actuators— better its dynamics, lower the actuator specifications for a given set of motion generation tasks. This view point may be termed as an "extrinsic" one, since it depends on the specification of the *trajectory*, which is independent of the design of the manipulator. For example, in [7], extrinsic measures such as the magnitude of the actuator/input torque and power in the worst case scenario, are directly used as indices for dynamic performance. A better alternative might be to look for *intrinsic* properties of the manipulator, which imparts upon it good dynamic performance, irrespective of the trajectory demanded of it. If such properties can be quantified in terms of indices, then such indices would be functions of the *architecture parameters* and the configuration of the manipulator alone. It is, therefore, possible to associate such an index, to each point of the workspace, so as to study the dynamic performance of a manipulator over a given finite region inside its workspace. Many indices have been proposed in literature towards this end, in the case of the serial manipulators. Asada analysed the isotropy of the Generalised Inertia Ellipsoid [8]. Yoshikawa proposed a measure to capture the dynamic performance [9]. Most of the indices proposed are based on the condition number of Generalised Inertia Matrix (GIM). In [10], [11] non-homogeneity in the task space is taken care of by studying the isotropy of the non-dimensional inertia matrix. Very few researchers have extended the concept of dynamic performance indices to parallel manipulators. For example, [12] introduced indices for analysing 3-degree-of-freedom parallel manipulators, but their correlation to the extrinsic measures are not established in literature.

In spite of the proliferation of different dynamic performance indices in literature, it is difficult to find ones which are intrinsic in nature, and yet, can predict the extrinsic behaviour. It is indeed non-trivial to formulate such indices in the case of dynamics, since the governing equation (i.e., the *equation of motion*) has two types of *rate variables*: velocities and accelerations. Furthermore, the velocities appear *quadratically* in the Coriolis and centripetal terms, leading to strong coupling between the different motion parameters. In order to define a meaningful measure, it is desirable to *decouple* the terms in multi-body dynamics first, so that some desirable property of the resulting system could be studied for the stated purpose. A measure for the extent of decoupling, termed as the *coefficient of coupling*, has been introduced in [13], and used for simplification of non-linear kinematic and dynamic coupling of robot dynamics.

In this work, a strategy is employed to decouple the equations of motion in a manner that the effect of Coriolis and centripetal terms, which are in correlation with that of the mass matrix, is reduced. This allows the study of the *mass matrix* alone using techniques from linear algebra. By studying the mass matrix, two intrinsic measures are developed which correlate with an extrinsic property, namely, the actuator torques required for the manipulator.

*kilarujagadeesh@iitm.ac.in
†muralikk@gmail.com
‡agr.saurav1@gmail.com
§sandipan@iitm.ac.in

Using the intrinsic measures defined as the two objectives and SWZ volume of the workspace as a constraint, a bi-objective optimisation problem is formulated to find designs fulfilling specific requirements. The optimisation problem is solved using NSGA-II [14], an optimiser based on genetic algorithms (GA). As GA uses a population-based approach, the computational demands for such an optimiser is rather high. To meet the high computational demands, a strategy exploiting the inherent parallelism in the objectives and constraint functions have been used, allowing for the use of GPU-based acceleration. To validate the proposed formulation, a planar parallel manipulator (PPM), namely the 3-<u>R</u>RR, is re-designed. The performance of the optimal design obtained is compared with the existing prototype available in the Robotics Laboratory, Department of Engineering Design, IIT Madras. The optimal design obtained shows improvements over its predecessor in terms of both the intrinsic performance indices, as expected. Moreover, such improvements seemingly correlate positively with the extrinsic performance index, such as the torque required to track the same set of representative trajectories—thus validating the main concept of the paper.

The rest of the paper is organised as follows: the formulation of the dynamic indices is introduced in Section II. The multi-objective optimisation problem is formulated in Section III, and the constraints, objectives and computational strategy used are elaborated. A case study is presented in Section IV using the PPM 3-<u>R</u>RR and the results are explained. The paper is concluded in Section V.

II. Dynamic performance indices

The equation of motion of a parallel manipulator can be written in the *actuator space* (see e.g., [15]) as:

$$M_{\theta}(q)\ddot{\theta} + C_{\theta}(q, \dot{q})\dot{\theta} + G_{\theta}(q) = \tau, \qquad (1)$$

where q is the set of generalised coordinates, M_{θ} is the mass matrix, θ is the vector of actuator space coordinates, C_{θ} represents the Coriolis and centripetal term and G_{θ} is the gravity term. Eq. (1) is fundamental in the analysis of the dynamic performance of a manipulator. As this equation involves two different types of *input-rate* variables, namely, the velocity $\dot{\theta}$, and the acceleration $\ddot{\theta}$, the dynamic performance of a manipulator cannot be quantified in the same way as its kinematic performance. In kinematics, it is customary to use a *unit speed* constraint [16] to *free* the intrinsic properties from the *scale effects* (i.e., study the properties of kinematics which do not depend on the input rates, but only on the geometry and configuration of the manipulator). While this cannot be done explicitly in the case of dynamics, one can observe that the effects of $\dot{\theta}$, and $\ddot{\theta}$ are not entirely different in the context of Eq. (1). For instance, the input speed, $\dot{\theta}$, occurs only in the second term $C_{\theta}\dot{\theta}$, which is qualitatively of the same nature as the first term $M_{\theta}\ddot{\theta}$ (as they both represent generalised forces).

Moreover, there is an innate relation between the terms M_{θ} and C_{θ}, which is explored in the following in such a manner that the transformation of the mass matrix M_{θ} modifies C_{θ} for the betterment of dynamic performance[1].

A. Relationship between the M and C matrices

It is known that the equation of motion of a conservative system can be derived from the *principle of least action* (see, e.g., [17]), i.e.,

$$\delta I = 0, \qquad (2)$$

where the *functional I* is given by the *action integral*:

$$I = \int_{t_1}^{t_2} L dt. \qquad (3)$$

In Eq. (3), L stands for the *Lagrangian* of the dynamic system under consideration. Focusing only on the *dynamic* terms (i.e., keeping the rate-independent term, potential energy out of consideration), $L = \frac{1}{2}\dot{\theta}^{\top}M(q)\dot{\theta}$. In such a case, one could write the equation of motion of a conservative system as:

$$\delta \int_{t_1}^{t_2} \frac{1}{2}\dot{\theta}^{\top}M(q)\dot{\theta}dt = 0. \qquad (4)$$

Eq. (4) leads to a differential equation of a particular form:

$$M_{ij}\ddot{\theta}_k + \Gamma_{ijk}\dot{\theta}_i\dot{\theta}_j = 0, \text{ where} \qquad (5)$$

$$\Gamma_{ijk} = \frac{1}{2}\left(\frac{\partial M_{ij}}{\partial \theta_k} + \frac{\partial M_{ik}}{\partial \theta_j} - \frac{\partial M_{kj}}{\partial \theta_i}\right), \; i, j, k = 1, \ldots, n,$$

where n is the degree-of-freedom (DoF) of the system. It may be noted that the terms Γ_{ijk} are functions of the configuration and architecture of the manipulator. The terms $\Gamma_{ijk}\dot{\theta}_i\dot{\theta}_j$, when summed up, generate the familiar term $C\dot{\theta}$ in the equation of motion. However, Γ_{ijk} can also be interpreted, from the perspective of *differential geometry*, as the *Christoffel symbols of the first kind* associated with the *metric tensor M* (see, e.g., [18] for more details on these topics). To understand the physical significance of the terms Γ_{ijk}, it is instructive to specialise Eq. (5) to the simple system of a particle of mass m, moving in $\mathbf{R}^n$. In such a case, one can show trivially:

$$M = m\mathbf{I}_{n \times n} \Rightarrow \Gamma_{ijk} = 0. \qquad (6)$$

where $\mathbf{I}_{n \times n}$ is an identity matrix of order n.

It is interesting to note the following:
• For a particle (of constant mass), the equation of motion, Eq. (5), coincides with the equation of the *geodesic* in $\mathbf{R}^n$ (i.e., $\ddot{\theta} = \mathbf{0}$). In other words, such a system has

---

[1]It may be noted here, that the third term in the equation of motion, namely, G_{θ}, is not considered in this work. It is the subject matter of a different study, namely, *static balancing* of manipulators and mechanisms.

the *best* dynamic behaviour, given that the system can *always* move along geodesic paths, which are the best possible, from a kinematic perspective.

• The vanishing of the Christoffel symbols in this case demonstrates the *flatness* of the configuration space $\mathbf{R}^n$, as well as the fact that the individual degree-of-freedom of the particle are completely *decoupled* in nature.

• When the Christoffel symbols are not all zeros, they relate to the non-zero *curvature* of the configuration space. It is consistent with the fact that in the equation of motion, they are associated with the Coriolis and centripetal accelerations. It is easy to see, in the case of the particle, that these accelerations appear only when there is a curvature in the path of the particle.

From these observations, one concludes that if the equation of motion of a system can be *made to appear* like that of a particle, then the system's dynamics would acquire the "particle-like" desirable properties, thereby motivating the indices for dynamic performance proposed in this study. Firstly, it is understood that if the mass matrix can be made isotropic, then it would reduce the coupling effects in the term $\boldsymbol{C_\theta}$ as well—resulting in greater uniformity of the dynamic behaviour over the configuration space, than can be expected otherwise. However, the isotropy by itself is not *sufficient* to ensure *faster* dynamic response (or equivalently, lower demands on the actuators for fast motions), which is also a desirable property from a practical perspective. To address this issue, one has to consider the repeated eigenvalues, λ, of the mass matrix. The value λ, being analogous to the "mass" of the equivalent particle, is the measure of the inertia of the reduced system. A similar measure, termed as the "swiftness ratio" has been used in [19], from similar considerations.

B. Development of the indices

In the following, two different indices are developed to take care of the two aspects of dynamics, as noted above. The first one is a non-dimensional one, which quantifies the deviation of a mass matrix from its diagonal form. The second index has the dimension of inertia, and it captures the equivalent inertia of the system.

To develop the first index, the condition number based on the L_1 norm is used. Given $\boldsymbol{A} \in \mathbf{R}^{n \times n}$, its condition number is given by

$$\kappa(\boldsymbol{A}) = \|\boldsymbol{A}^{-1}\|\|\boldsymbol{A}\|, \text{ where} \tag{7}$$

$$\|\boldsymbol{A}\|_{L_1} = \sum_{i=1}^{n}\sum_{j=1}^{n} |x_{ij}|. \tag{8}$$

Mass matrix, $\boldsymbol{M_\theta} \in \mathbf{R}^{n \times n}$, can be transformed to its diagonal form $\boldsymbol{\Lambda}$, where $\boldsymbol{\Lambda}$ is matrix of the eigenvalues of $\boldsymbol{M_\theta}$. Since $\boldsymbol{M_\theta}$ is positive semi-definite, Eq. (8) reduces to:

$$\|\boldsymbol{\Lambda}\|_{L_1} = \sum_{i=1}^{n} \lambda_i, \tag{9}$$

where λ_i are the eigenvalues of $\boldsymbol{M_\theta}$. Therefore, the constraint on the workspace to be inside SWZ is imperative. Using Eq. (9), the condition number of $\boldsymbol{\Lambda}$ can be written as:

$$\kappa_{L_1}(\boldsymbol{\Lambda}) = \left(\frac{1}{\lambda_1} + \cdots + \frac{1}{\lambda_n}\right)(\lambda_1 + \cdots + \lambda_n). \tag{10}$$

Using κ_{L_1}, the dynamic performance index $\mu_1(\boldsymbol{M_\theta})$ is defined as:

$$\mu_1(\boldsymbol{M_\theta}) = \frac{n^2}{\kappa_{L_1}(\boldsymbol{\Lambda})}, \text{ such that } \mu_1(\boldsymbol{M_\theta}) \in [0, 1]. \tag{11}$$

As the value of $\mu_1(\boldsymbol{M_\theta})$ approaches unity, eigenvalues of the mass matrix approach each other, i.e., the mass matrix $\boldsymbol{M_\theta}$ approaches isotropy. At an isotropy, $\lambda_{max} = \lambda_{min} = \lambda$, and hence, $\boldsymbol{\Lambda} = \lambda \boldsymbol{I}_{n \times n}$. Therefore,

$$\begin{aligned}\boldsymbol{M_\theta} &= \boldsymbol{Q}\boldsymbol{\Lambda}\boldsymbol{Q}^\top, \text{ where } \boldsymbol{Q}\boldsymbol{Q}^\top = \boldsymbol{I}_{n \times n} \\ &= \lambda\boldsymbol{Q}\boldsymbol{Q}^\top \\ &= \lambda\boldsymbol{I}_{n \times n}.\end{aligned} \tag{12}$$

From Eq. (12) one can observe that the isotropy ensures diagonality, i.e., complete decoupling of the inertia term, and it is not necessary to consider their decoupling separately. The norm mentioned in Eq. (8) is chosen because of its simplicity, ease of computation, and to represent the index in terms of matrix invariants. For example, the isotropy index, μ_1, for the three degree-of-freedom 3-RRR PPM can be written in terms of their invariants using Eq. (10) and Eq. (11) as:

$$\begin{aligned}\mu_1(\boldsymbol{M_\theta}) &= \frac{9}{\kappa_{L_1}(\boldsymbol{\Lambda})} & (13) \\ &= \frac{9}{\left(\frac{1}{\lambda_1} + \frac{1}{\lambda_2} + \frac{1}{\lambda_3}\right)(\lambda_1 + \lambda_2 + \lambda_3)} \\ &= \frac{9\lambda_1\lambda_2\lambda_3}{(\lambda_1 + \lambda_2 + \lambda_3)(\lambda_1\lambda_2 + \lambda_2\lambda_3 + \lambda_1\lambda_3)} \\ &= \frac{9I_3(\boldsymbol{M_\theta})}{I_1(\boldsymbol{M_\theta})I_2(\boldsymbol{M_\theta})},\end{aligned}$$

where $I_1(\boldsymbol{M_\theta}) = \text{tr}(\boldsymbol{M_\theta})$, $I_2(\boldsymbol{M_\theta}) = \frac{1}{2}((\text{tr}(\boldsymbol{M_\theta}))^2 - \text{tr}(\boldsymbol{M_\theta}^2))$, and $I_3(\boldsymbol{M_\theta}) = \det(\boldsymbol{M_\theta})$ are the invariants of mass matrix $\boldsymbol{M_\theta}$. Similarly, this can be extended to matrices of higher orders.

The second index involves the eigenvalues of the mass matrix. It is defined simply as

$$\mu_2(\boldsymbol{M_\theta}) = \max\{\lambda_i\}, \ i = 1, \ldots, n. \tag{14}$$

The indices $\mu_1(\boldsymbol{M_\theta})$, $\mu_2(\boldsymbol{M_\theta})$ are both *local* in nature, as the mass matrix itself varies over the configuration space. To extend these to global indices over a workspace of interest, the following strategies are employed.

1. Using the average value of the index μ_1 over the workspace of interest (V), a global index, $\bar{\mu}_1$, is defined:

$$\bar{\mu}_1(\boldsymbol{M_\theta}) = \frac{\int_V \mu_1(\boldsymbol{M_\theta}) dv}{\int_V dv}. \qquad (15)$$

2. It is of interest to find the design parameters such that the maximum equivalent inertia, considered over the desired range of motion (i.e., workspace of interest, W), is minimised. Therefore, another global index, $\bar{\mu}_2$ is defined:

$$\bar{\mu}_2 = \max_W(\mu_2) = \max_W(\lambda_{max}(\boldsymbol{M_\theta})). \qquad (16)$$

III. Formulation of the optimisation problem and computational scheme

Design problem of a parallel manipulator is inherently multi-objective in nature (as explained above), and hence requires computation of many functions, such as the size of the SWZ, computation of dynamic performance index, isotropy, dexterity etc., which are often computationally expensive and not known analytically. It may not be possible to find the gradient of all these functions at every point, precluding the use of gradient-based local techniques to solve the optimisation problem. Genetic Algorithms (GA), employed for optimisation in the present work, can handle such multi-objective optimisation problems. In order to eliminate the need of a "good" initial guess, and to explore a search space better, the GA uses a *population-based approach* and optimises iteratively over *generations*. In this section, the formulation of the objective functions and the constraints used in the optimisation are described, and their implementation in NSGA-II[2] [14] is explained. A computational scheme is presented to exploit the inherent parallelism in the evaluation of the objective functions over a search space and its implementation in GPU for faster computations is demonstrated.

A. Objective functions and constraints

The objective functions and constraints for the problem are motivated from the idea that a manipulator should have a desired SWZ and it should also have a good dynamic performance over the SWZ. Two different design objectives— large $\bar{\mu}_1$ and small $\bar{\mu}_2$—are considered in this work. The constraint function, $g(\boldsymbol{x})$, is chosen based on the minimum dimension of the SWZ[3] denoted as ρ_o. The optimisation problem can be written as:

$$
\begin{aligned}
\text{Minimise} \quad & f_1(\boldsymbol{x}) = -\bar{\mu}_1 \quad \text{and} \\
& f_2(\boldsymbol{x}) = \bar{\mu}_2 \\
\text{subject to} \quad & g(\boldsymbol{x}) : \rho - \rho_o \geq 0, \\
& x_j \in [a_j, b_j], \quad j = 1, \dots, k. \quad (17)
\end{aligned}
$$

where k is the number of design parameters.

[3]The mass matrix ($\boldsymbol{M_\theta}$) is defined only at a non-singular configuration. Hence, it is imperative to confine the domain of analysis to the SWZ.

B. SWZ computation

To identify the usable workspace of a manipulator, the concept of SWZ [6] is used in the present work. The computation of SWZ involves evaluation of the level-sets of various functions, S_i, which comprise of conditions for loss-type singularities, gain-type singularities, joint limits and link interference functions, are non-analytic in nature requiring evaluation over the entire search space. To find their zero level-sets, the search space is divided using a polar grid and each function, S_i, is evaluated at the grid points. The centre of the grid corresponds to that of the centre of symmetry of the manipulator (e.g., $\boldsymbol{o}$ in Fig. 1). The resolution of the search/grid space is determined based on the desired accuracy of the solutions in task-space and a higher accuracy demands more computation. As the evaluation of a function at a grid point is independent of the evaluation at the other points, the entire computation is parallelised and GPU[4] is used. The scheme affords for large population sizes and higher number of generations for NSGA-II runs.

IV. Case Study: 3-RRR planar parallel manipulator

The optimisation strategy described in Section III is applied to a symmetric 3-DoF planar parallel manipulator, 3-RRR, shown in Fig. 1. The base points, $\boldsymbol{b}_1$, $\boldsymbol{b}_2$, and $\boldsymbol{b}_3$, describe an equilateral triangle of side b and define the locations of the actuators. The end-effector is of the form of an equilateral triangle of side a, with the vertices $\boldsymbol{p}_1$, $\boldsymbol{p}_2$, and $\boldsymbol{p}_3$. The pair of points $\boldsymbol{b}_i$ and $\boldsymbol{p}_i$ ($i = 1, 2, 3$), are connected by a RR chain each. The first link, $\boldsymbol{b}_i\boldsymbol{a}_i$, in each chain, is the *active* link of length l. Similarly, the second link, $\boldsymbol{a}_i\boldsymbol{p}_i$, in each chain is a *passive* link of length r. The actuator variables are $\boldsymbol{\theta} = (\theta_1, \theta_2, \theta_3)^\top$ and the passive variables $\boldsymbol{\phi} = (\phi_1, \phi_2, \phi_3)^\top$, while the task space variables are $\boldsymbol{\mathcal{X}} = (x, y, \alpha)^\top$.

The active links, the passive links, and the moving platform are in three different parallel planes to avoid collisions amongst them. Further, each leg of the 3-RRR has two inverse kinematics branches. Here each leg is considered in the same branch of inverse kinematics to maintain symmetry. Among the two symmetric branches, the branch shown in Fig. 1 is chosen without any loss of generality, as the two branches are equivalent with regard to their dynamics.

It has to be noted that dynamic model of the PPM is dependent on the architecture parameters of the links. To capture and simplify this dependence, the complete geometric model of the link is parameterised in terms of its link length by using three dimensional geometric primitives such as, cylinders, cuboids, triangular prisms etc. A close approximation to an actual link of 3-RRR PPM is obtained by maintaining high packing efficiency. Density of the material and the payload are then incorporated to complete the

[4]The GPU used is NVIDIA Tesla K40 with an Intel® Core i7-4770 CPU @ 3.40GHz processor with 8GB of RAM and the codes are written in CUDA C.
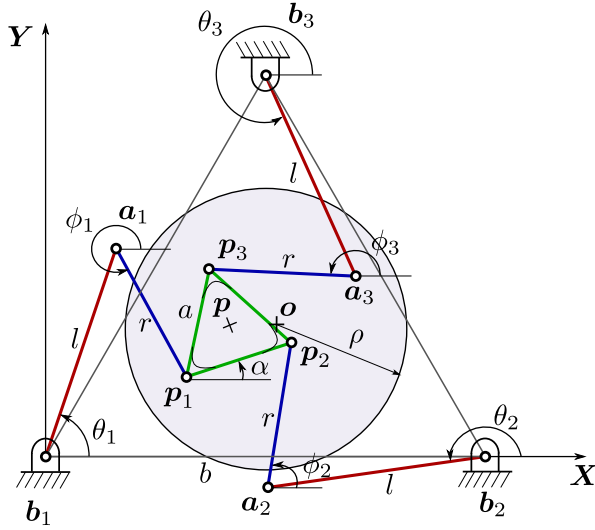
Fig. 1. Kinematic details of a 3-R̲RR planar parallel manipulator.

dynamic model. For example, link design of the PPM is shown in Fig. 2. Each of the dimensions, b_1, h_1, etc., are functions of the length, l, making l the sole "free" variable entering the design space. All the lateral dimensions are related to l in such a manner that the *flexural stiffness* of the links remain unchanged even when the length is varied.
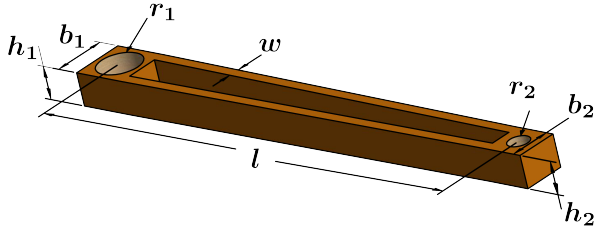

Fig. 2. The CAD model of an active link of 3-R̲RR showing its geometric parameters

A. Design variables

As described in [6], SWZ of the 3-R̲RR manipulator is computed to obtain a cylinder free from singularities and link interferences. A three-dimensional grid is considered such that each axis represents a DoF in the task-space. A right circular cylinder is fitted and is placed at the centre of the manipulator (o) with height $2\Delta\alpha$. The SWZ is found for discrete values of α, with a range of $\alpha_{mid} \pm \Delta\alpha$, based on the desired resolution. The radius of the cylinder is taken as a measure for SWZ, denoted by ρ as shown in Fig. 1.

The equation of motion for a 3-R̲RR PPM can be derived in task space, as given in Eq. (1), with task-space variables as $\boldsymbol{\mathcal{X}} = (x, y, \alpha)^\top$. In this work the PPM is designed for axis-symmetric jobs like welding, laser cutting etc., allowing the use of the orientation as a "free design" parameter

for improving dynamics in the other two directions. The dynamic indices $\bar{\mu}_1$ and $\bar{\mu}_2$, described in Section II, are evaluated using the actuator space mass matrix $\boldsymbol{M_\theta}$.

The optimisation problem is formulated as described in Section III-A, with the design variable as $\boldsymbol{x} = (b, l, r, a, \alpha_{mid})^\top$. The ranges of the design variables and values of the fixed parameters are listed in Table I and Table II, respectively.

TABLE I. Ranges of the design variables for the optimisation of 3-R̲RR PPM

Variable	Lower bound	Upper bound
b	400 mm	1000 mm
l	100 mm	500 mm
r	100 mm	500 mm
a	50 mm	500 mm
α_{mid}	$-175°$	$175°$

TABLE II. Fixed parameters for the optimisation of 3-R̲RR PPM

Parameter	Value
ρ_o	300 mm
$\Delta\alpha$	5°
Payload	1 kg
Density	2.710×10^{-3} kg/mm^3

B. Results

Optimal designs are found using NSGA-II with the chosen parameters given in Table III and population size of 600 over 200 generations. The number of generations is chosen to be relatively low, as it is found to suffice for the convergence of the results, with a seed value of 0.5. The task-

TABLE III. Internal control parameters for NSGA-II

Parameter	Value
p_c	0.90
p_m	0.50
η_c	5
η_m	35

space is discretised at a resolution of 0.125 mm and 0.5° for the computation of SWZ. A total time of 4 hours was taken to complete the optimisation. The result obtained from NSGA-II is studied by means of the Pareto plot, shown in Fig. 3. For a more detailed study, three designs are chosen from the Pareto plot—minimum $\bar{\mu}_2$ point as design-a, *utopia point* as design-b, and maximum $\bar{\mu}_1$ point
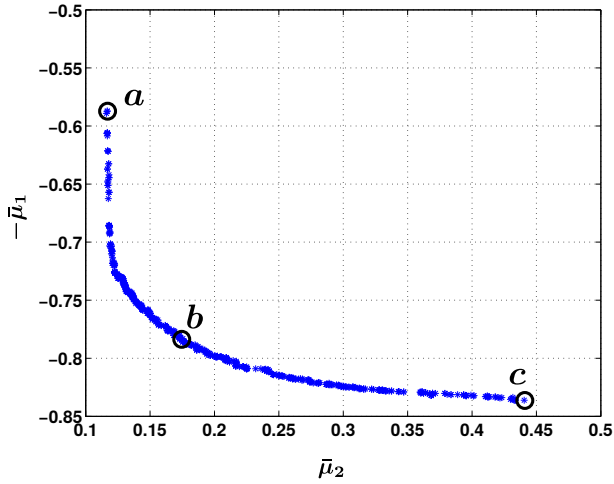
Fig. 3. Pareto plot for optimisation of 3-RRR PPM based on $\bar{\mu}_1$ and $\bar{\mu}_2$

Due to constraint of space, only the torques demanded of the first actuator (located at b_1), are presented in Fig. 5. However, a similar trend is observed for all the results. As seen in Table V, the peak torques in the case of design-a are reduced by 50% compared to the existing design.

TABLE V. Indices ($\bar{\mu}_1$, $\bar{\mu}_2$) and absolute peak torque values (τ_p)

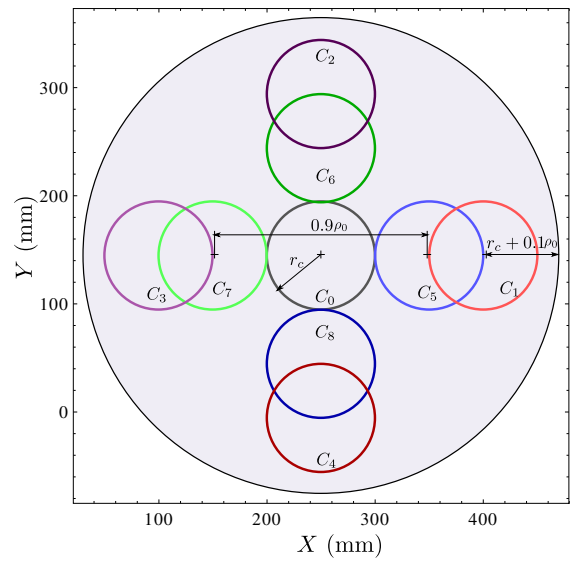| Design	$\bar{\mu}_1$	$\bar{\mu}_2$ (kg-m^2)	τ_p(Nm) $u = 1$ m/s	τ_p(Nm) $u = 1.5$ m/s
Existing	0.48	1.19	16.4	37.6
Proposed	0.58	0.12	8.3	19.0

Fig. 4. Schematic of the nine circular paths, $C_i, i = 0, \dots, 8$, traced by the end-effector. The shaded circular region represents the SWZ for $\alpha = \alpha_{mid}$.

as design-c, shown in Fig. 3. It has been observed that the magnitude of the maximum torque does not vary significantly over the different designs. To quantify the benefits afforded by the optimisation, the optimal design is compared with an existing prototype, which was constructed without such considerations. The design variables of the two cases are given in Table IV. Another observation is that the value of r reaches its upper limit of 500 mm to accommodate the required SWZ.

In order to validate the design improvement from an extrinsic perspective, the actuator torques are computed, as the manipulator tracks different paths distributed over the SWZ. A circular path with radius $r_c = 50$ mm is chosen. The point, p, is made to trace the path with constant speeds of $u = 1$ m/s and $u = 1.5$ m/s. The analysis is carried out for the fixed orientation (α is used as design variable) of the end-effector, $\alpha = \alpha_{mid}$, throughout the trajectory, for each selected design. Nine such paths, $C_i, i = 0, \dots, 8$, as shown in Fig. 4, are distributed over the SWZ.

V. Conclusion

A novel approach to the quantification of the dynamic performance of a parallel manipulator has been defined in this paper. Two new indices have been proposed, based entirely on the intrinsic properties of the system. The locally-defined indices have been extended to two physically meaningful global indices, which are then utilised to define the objective functions of a multi-objective design problem. Using the example of a planar 3-RRR manipulator, such a design problem is solved, with the additional constraint of a given SWZ. The results show that the method leads to better designs of the manipulator, which perform better not just in theory, but also in practice—from the perspective of required actuator efforts to track a given trajectory. The proposed indices, formulation, and solution, though demonstrated here using a solitary example, can potentially be applied to any parallel manipulator.
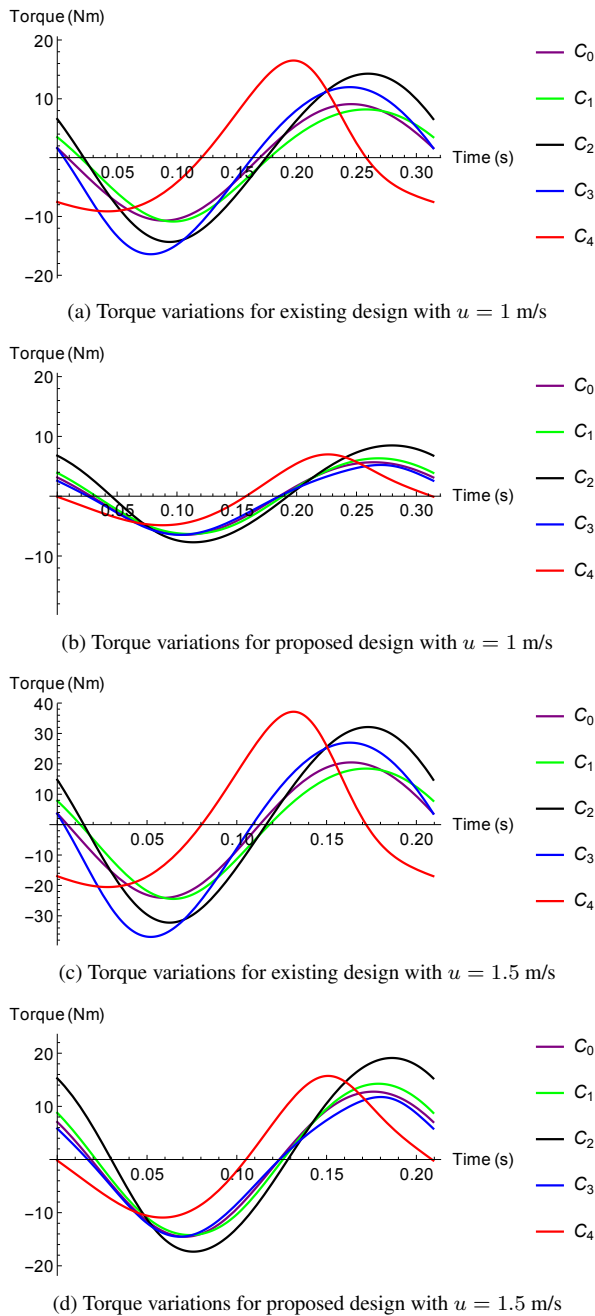
TABLE IV. Values of variables for existing and proposed design

Parameter	Existing Design	Proposed design (rounded off)
b (mm)	1000	**938**
l (mm)	500	**307**
r (mm)	500	**500**
a (mm)	150	**136**
α_{mid}	68°	**62°**
$\bar{\mu}_1$	0.48	**0.58**
$\bar{\mu}_2$	1.19	**0.12**

(a) Torque variations for existing design with $u = 1$ m/s

(b) Torque variations for proposed design with $u = 1$ m/s

(c) Torque variations for existing design with $u = 1.5$ m/s

(d) Torque variations for proposed design with $u = 1.5$ m/s

Fig. 5. Torque variations in actuator at $\boldsymbol{b}_1$ for the designs given in Table IV. Each plot shows the torques for five different paths

ACKNOWLEDGEMENT

References

[1] M. K. Lee and K. W. Park, "Kinematic and dynamic analysis of a double parallel manipulator for enlarging workspace and avoiding singularities," *Robotics and Automation, IEEE Transactions on*, vol. 15, no. 6, pp. 1024–1034, Dec 1999.

[2] Y. Li, J. Wang, X.-J. Liu, and L.-P. Wang, "Dynamic performance comparison and counterweight optimization of two 3-DoF parallel manipulators for a new hybrid machine tool," *Mechanism and Machine Theory*, vol. 45, no. 11, pp. 1668 – 1680, 2010.

[3] L. Wang, J. Wu, and J. Wang, "Dynamic formulation of a planar 3-DoF parallel manipulator with actuation redundancy," *Robotics and Computer-Integrated Manufacturing*, vol. 26, no. 1, pp. 67 – 73, 2010.

[4] T. Huang, S. Liu, J. Mei, and D. G. Chetwynd, "Optimal design of a 2-DoF pick-and-place parallel robot using dynamic performance indices and angular constraints," *Mechanism and Machine Theory*, vol. 70, pp. 246 – 253, 2013.

[5] G. Wu, "Multiobjective Optimum Design of a 3-RRR Spherical Parallel Manipulator with Kinematic and Dynamic Dexterities," *Modeling, Identification and Control*, vol. 33, no. 3, pp. 111–121, 2012.

[6] R. A. Srivatsan and S. Bandyopadhyay, "Determination of the safe working zone of a parallel manipulator," in *Computational Kinematics*, ser. Mechanisms and Machine Science, F. Thomas and A. Perez Gracia, Eds. Springer Netherlands, 2014, vol. 15, pp. 201–208.

[7] Y. Zhao, "Dynamic optimum design of a three translational degrees of freedom parallel robot while considering anisotropic property," *Robotics and Computer-Integrated Manufacturing*, vol. 29, no. 4, pp. 100–112, 2013.

[8] H. Asada, "A geometrical representation of manipulator dynamics and its application to arm design," *Journal of dynamic systems, measurement, and control*, vol. 105, no. 3, pp. 131–142, 1983.

[9] T. Yoshikawa, "Dynamic manipulability of robot manipulators," in *Robotics and Automation. Proceedings. 1985 IEEE International Conference on*, vol. 2, Mar 1985, pp. 1033–1038.

[10] O. Ma and J. Angeles, "The concept of dynamic isotropy and its applications to inverse kinematics and trajectory planning," in *Robotics and Automation, 1990. Proceedings., 1990 IEEE International Conference on*, May 1990, pp. 481–486 vol.1.

[11] A. Bowling and O. Khatib, "The dynamic capability equations: a new tool for analyzing robotic manipulator performance," *Robotics, IEEE Transactions on*, vol. 21, no. 1, pp. 115–123, Feb 2005.

[12] R. Di Gregorio and V. Parenti-Castelli, "Dynamic performance indices for 3-dof parallel manipulators," in *Advances in Robot Kinematics*, J. Lenari and F. Thomas, Eds. Springer Netherlands, 2002, pp. 11–20.

[13] V. D. Tourassis and C. P. Neuman, "The inertial characteristics of dynamic robot models," *Mechanism and Machine Theory*, vol. 20, no. 1, pp. 41 – 52, 1985.

[14] K. Deb, A. Pratap, S. Agarwal, and T. Meyarivan, "A fast and elitist multiobjective genetic algorithm: NSGA-II," *Evolutionary Computation, IEEE Transactions on*, vol. 6, no. 2, pp. 182–197, April 2002.

[15] C. Nasa and S. Bandyopadhyay, "Trajectory-tracking control of a planar 3-RRR parallel manipulator with singularity avoidance," in *Robotics and Mechatronics, 13th World Congress in Mechanism and Machine Science, Robotics and Mechatronics, Mexico*, 2011, pp. 19–25.

[16] A. Ghosal and B. Ravani, "A differential-geometric analysis of singularities of point trajectories of serial and parallel manipulators," *Trans. of ASME, Journal of Mechanical Design*, vol. 123, no. 1, pp. 80–89, March 2001.

[17] H. Goldstein, C. P. Poole, and J. L. Safko, *Classical Mechanics*. Addison Wesley, 2001.

[18] R. S. Millman and G. D. Parker, *Elements of Differential Geometry*. Prentice-Hall Inc., 1977.

[19] R. Gregorio and V. Parenti-Castelli, "On the characterization of the dynamic performances of planar manipulators," *Meccanica*, vol. 40, no. 3, pp. 267–279, 2005.